



Climate impacts on the structures of the North Pacific air-sea CO₂ flux variability

V. Valsala¹, S. Maksyutov², M. Telszewski³, S. Nakaoka², Y. Nojiri², M. Ikeda⁴, and R. Murtugudde⁵

¹Indian Institute of Tropical Meteorology (IITM), Pune, India

²CGER, National Institute for Environmental Studies (NIES), Tsukuba, Japan

³Intergovernmental Oceanographic Commission of UNESCO, Paris, France

⁴Retired from EES, Hokkaido University, Japan

⁵ESSIC, University of Maryland, College Park, Maryland, USA

Correspondence to: V. Valsala (valsala@tropmet.res.in)

Received: 5 April 2011 – Published in Biogeosciences Discuss.: 2 May 2011

Revised: 2 January 2012 – Accepted: 5 January 2012 – Published: 25 January 2012

Abstract. Some dominant spatial and temporal structures of the North Pacific air-sea CO₂ fluxes in response to the Pacific Decadal Oscillation (PDO) are identified in three data products from three independent sources: an assimilated CO₂ flux product and two forward model solutions. The interannual variability of CO₂ flux is found to be an order of magnitude weaker compared to the seasonal cycle of CO₂ flux in the North Pacific. A statistical approach is employed to quantify the signal-to-noise ratio in the reconstructed dataset to delineate the representativity errors. The dominant variability with a signal-to-noise ratio above one is identified and its correlations with PDO are examined. A tentative four-pole pattern in the North Pacific air-sea CO₂ flux variability linked to PDO emerges in which two positively correlated poles are oriented in the northwest and southeast directions and contrarily, the negatively correlated poles are oriented in the northeast and southwest directions. This pattern is identified in three products, providing CO₂ and *p*CO₂. Its relations to the interannual El Niño-Southern Oscillation (ENSO) and lower-frequency PDO are separately identified. A combined EOF analysis between air-sea CO₂ flux and key variables representing ocean-atmosphere interactions is carried out to elicit robust oscillations in the North Pacific CO₂ flux in response to the PDO. The proposed spatial and temporal structures of the North Pacific CO₂ fluxes are insightful since they separate the secular trends of the surface ocean carbon from the interannual variability. The regional characterization of the North Pacific in terms of PDO and CO₂ flux variability is also instructive for determining the homogeneous oceanic domains for the Regional Carbon Cycle and Assessment Processes (RECCAP).

1 Introduction

The ocean absorbs nearly one third of the anthropogenic CO₂ from the atmosphere via air-sea gas exchange (Gruber et al., 2009). The ocean's uptake of anthropogenic CO₂ has significantly contributed to the mitigation of the net growth of CO₂ in the atmosphere. The annual mean value of oceanic sink of CO₂ was nearly zero during the pre-industrial era (i.e., when the atmospheric CO₂ concentration was at 273 parts per million; ppm) and rose fairly rapidly to above 1.5 Peta gram of carbon (PgC; i.e., when the atmospheric CO₂ concentration rose to over 380 ppm and continues to rise). The contemporary CO₂ sink of the ocean, which includes both natural and anthropogenic fractions, is estimated to be between 1.5 and 2.2 PgC (e.g., Takahashi et al., 2009; Gruber et al., 2009, Le Quéré et al., 2007).

The oceanic sinks of CO₂ respond to climate anomalies. In addition to the climate induced variability, secular trends in the sinks due to the accumulation of CO₂ in the atmosphere cause significant deviations in the annual mean value mentioned above. From previous studies, it has been estimated that 70 % of the interannual variability of contemporary air-sea CO₂ fluxes is driven by the cycles of El Niño-Southern Oscillation (ENSO) in the Pacific, namely a positive sink or an anomalous reduction in oceanic outgassing of ~0.5 PgC during El Niño years (Valsala and Maksyutov, 2010; Gruber et al., 2009; McKinley et al., 2004; Obata and Kitamura, 2003; Le Quéré et al., 2000). It should be noted that ENSO has a global reach in terms of temperature and precipitation teleconnections and the phasing of marine vs. terrestrial sources/sinks have yet to be fully understood (Jones et al., 2001). The majority of the remaining variability in CO₂ sink

is driven by the Southern Annular Mode (SAM; Le Quéré et al., 2007; Lovenduski et al., 2007). In addition to this interannual variability, the contemporary air-sea CO₂ fluxes also show interdecadal variability related to the Pacific Decadal Oscillation (PDO; see Latif and Barnett, 1994 and Mantua et al., 1997) and the North Atlantic Oscillation (NAO; see Hurrell, 1995 for NAO; impacts on oceanic carbon cycle are reported by several studies – Thomas et al., 2008; McKinley et al., 2004; Patra et al., 2005). Moreover, because of the accumulation of CO₂ in the atmosphere and subsequent changes in the dynamics of the atmosphere and the ocean, regional air-sea CO₂ fluxes also display clear trends (Le Quéré et al., 2009; Le Quéré et al., 2007).

The above conclusions on interannual variability of air-sea CO₂ fluxes are drawn mainly from simulations of simple-to-intermediate complexity, state-of-the-art, biogeochemical general circulation models (BGCs). A few studies have validated these results with data-model intercomparisons based on available observations. For instance, the general conclusions on ENSO and air-sea CO₂ flux relations in the tropical Pacific were observationally verified by Feely et al. (2002; also see Christian et al., 2008). Similarly, the southern ocean trends of CO₂ emissions are also backed by observations in the work of Le Quéré et al. (2007) and Metzl et al. (2006). However, the limited number of observations in terms of spatial and temporal dimensions make it rather difficult to determine the robustness of these conclusions, especially when one wants to separate the effect of interannual to interdecadal variability from the secular trends or delineate the impacts of ocean dynamics (e.g., thermocline variability) and thermodynamics (mixed layer and sea surface temperature variability) on air-sea CO₂ and sea water partial pressure of CO₂ (*p*CO₂) variations.

The methods for estimating air-sea CO₂ fluxes on global scale can be generally categorized as follows: (1) Direct observations of global surface ocean *p*CO₂ are interpolated onto the global domain and the products typically include climatological maps of air-sea CO₂ fluxes, as in the database of Takahashi et al. (2009). Due to the limited number of observations of *p*CO₂ especially at interannual time scales, this method does not yield the vital information regarding the interannual to interdecadal variability of air-sea CO₂ fluxes. (2) State-of-the-art BGCs incorporating ecosystem models of varying complexities are employed in order to simulate global ocean CO₂ fluxes on interannual to interdecadal time scales (Christian et al., 2008; McKinley et al., 2004; Obata and Kitamura, 2003; Le Quéré et al., 2000). (3) Inverse estimations are made from transports of atmospheric CO₂ concentrations and are utilized to generate global air-sea CO₂ fluxes on interannual time scales (Patra et al., 2005; Gurney et al. 2004, Rödenbeck et al., 2003). However the regional patterns of interannual variability are poorly resolved in these rather coarse resolution inversion systems (Gurney et al., 2004). (4) The BGCs as well as atmospheric transport models are optimized with various sets of observations

and a robust estimation of air-sea CO₂ fluxes is attempted (Valsala and Maksyutov, 2010; Tjiputra et al., 2007; Baker et al., 2006). (5) The empirical relations between certain surface ocean parameters and *p*CO₂ are exploited in order to infer the *p*CO₂ on interannual time scales (Park et al., 2010; Telszewski et al., 2009). In this study, we use air-sea CO₂ fluxes estimated with some of the methods discussed above and examine the patterns of interannual variability of North Pacific CO₂ fluxes and the possible climatic control from interannual (ENSO) to decadal (PDO) time-scales.

A most comprehensive and commendable study on the interannual variability of air-sea CO₂ fluxes in the North Pacific and its linkage to PDO was carried out by McKinley et al. (2006). In their study, they compared results from seven biogeochemical models, each of them with a varying complexity of ecosystem models, and examined the interannual variability of North Pacific air-sea CO₂ fluxes. A major conclusion of their study was that the magnitude of low-frequency air-sea CO₂ flux variability in the North Pacific is relatively small, with a maximum of amplitude of 0.025 PgC/yr related to PDO. The reason for such a weak decadal variability is that the effect of decadal sea surface temperature (SST), dynamics of dissolved inorganic carbon (DIC) as well as alkalinity on *p*CO₂ are opposite in phase and similar in magnitude. Therefore, the net change in *p*CO₂ due to the sum of partial changes induced by above three factors nearly cancel each other leaving a relatively small net residual of interannual *p*CO₂ anomalies (and thereby a weak interannual air-sea CO₂ flux anomaly as well). Even though the net interannual variability naturally appears as a small residual of the above controlling factors, it is still worth considering because such anomalies should be separated first from the secular trends related to the natural modes of variability in order to assess the growth rate of CO₂ in the ocean due to anthropogenic forcing. This is also critical for understanding the response of this important region to continued anthropogenic forcing.

Takahashi et al. (2006) reported the trends of surface ocean *p*CO₂ in the North Pacific as it was compiled from 30-years of available observations. The study identified that except for the Bering and Okhotsk Seas, the *p*CO₂ values corresponding to the in-situ SST increased at a mean decadal rate of nearly 10 µatm. In another study Midorikawa et al. (2006a) focused on the long term trend of CO₂ along the 137° E longitude line. They identified a persistent increase of CO₂ by the atmospheric inputs at a rate of nearly 1 µatm yr⁻¹. Studies by Wakita et al. (2010) also looked at the DIC increase in the western North Pacific based on observational analysis. In these vital studies (based on observations) the regional tendency of oceanic CO₂ and its decadal variability are addressed. Our study, on the other hand, nicely complements these previous studies with detailed regional structures of North Pacific CO₂ variability, especially by filling the gaps where previous observation based studies could not resolve the spatial variability completely.

A few other notable studies which are based on observational data analysis of North Pacific CO₂ fluxes, identified that the contrasting effects between SST and DIC anomalies cause small *p*CO₂ variations in the subtropical gyre north of 23° N (Midorikawa et al., 2006b). The general circulation model results of McKinley et al. (2006) are broadly consistent with this result. Midorikawa et al. (2006a) focused on the interannual variability of the winter time oceanic CO₂ and air-sea CO₂ fluxes in the western North Pacific based on 2 decades of observations made along 137° E. They found positive correlations between DIC and the decadal variability in the North Pacific identified as North Pacific Index with a time lag of 2 years from 15° N to 18° N and with a time lag of 3 years for 11° N to 14° N and reported an influence of large scale climate shift on the DIC variations and subsequent *p*CO₂ variations in these regions.

Although the study by McKinley et al. (2006) was quite comprehensive, in the sense that it assembled the results from seven biogeochemical models, the conclusions drawn thereby were fairly general. The study was based on a suite of forced ocean models with very little direct comparison with observations. Moreover, the study lacked the presentation of a close look into the spatio-temporal variability of the North Pacific air-sea CO₂ fluxes with respect to PDO. This is important to investigate because the crucial information for identifying the secular trends of CO₂ in the ocean from the sparse observations is even more important in the context of global warming and its potential impacts on ocean's ability to take up CO₂. It is important to avoid confusing such trend analysis with the natural interannual to interdecadal variability of CO₂ fluxes. To identify the regional patterns of the North Pacific CO₂ fluxes in response to PDO is the major goal of our study. We also strive to quantify the dynamical and thermodynamical contributions to the net CO₂ variability. Much attention has been focused on the impact of PDO on ecosystem responses in terms of regime shifts (for ex., Chavez et al., 2002; Mantua et al., 1997) and the role of bottom-up (circulation changes) vs. top-down (anthropogenic effect via fisheries, for ex., Lehodey et al. 2009) are basically unresolved. A similar issue remains for the carbon cycle in terms of the role of the thermocline variability as a bottom up forcing or dynamical driver for air-sea CO₂ flux variability vs. the surface mixed layer variability or the thermodynamic driver for *p*CO₂ and air-sea exchanges of CO₂. Anthropogenic CO₂ forcing is clearly confounded in this case with the global warming impact on the circulation itself and we will not attempt here to untangle the direct and indirect anthropogenic forcing of CO₂ variability.

The analysis presented here will also facilitate the assessment of the total carbon budget and its interannual-to-decadal variability which is a focus of the Regional Carbon Cycle and Assessment Processes (RECCAP). The RECCAP focuses on quantifying the interannual variability of regional carbon fluxes over land and the oceans where partitioning into different regions is accomplished by the prior knowledge about

the expected CO₂ flux variability. Therefore our study should offer highly relevant insights into regional specificities of interannual variability related to climate mode anomalies that should be targeted.

The following is the structure of the remaining parts of this paper. In Sect. 2 we describe the data and methods used. In Sect. 3 we propose a regional structure of North Pacific air-sea CO₂ fluxes in response to the PDO through correlation, partial correlation and singular value decomposition analyses. The results are discussed and concluding thoughts are offered in Sect. 4.

2 Data and methods

In this study we mainly use an optimized estimate of the air-sea CO₂ flux for 25 years spanning the period 1980–2004, based on a model with data assimilation which is derived from the work of Valsala and Maksyutov (2010, hereinafter referred to as OTTM). The total span of assimilation involved in OTTM is from 1996 to 2004. Prior to this period, interannual anomalies from the forward model are added to the seasonal climatology from the assimilation period of 1996–2004. In addition to this product, we also use air-sea CO₂ fluxes from two independent sources for comparison purpose and they are taken from McKinley et al. (2004a), spanning 1980–1999 and Le Quéré et al. (2005), over 1980–2004. These two products are from simulations of BGCMS.

The model details and the method of CO₂ flux estimations are described in their respective papers and therefore only a brief summary for each data set is provided here. The optimized air-sea CO₂ fluxes of OTTM are derived from a variational assimilation of surface ocean *p*CO₂ observations into a relatively simple biogeochemical model. This model comprises of an offline tracer transport model (Valsala et al., 2008) and a phosphate dependent ecosystem model based on McKinley et al. (2004a). A variational assimilation is used to constrain the surface ocean model *p*CO₂ using corresponding ship track observations from the database of Takahashi et al. (2007). The seasonal to interannual *p*CO₂ are assimilated by applying separate weights based on the model interannual variance. The details of the assimilation, error estimates and comparison with observational climatology of Takahashi et al. (2009) can be found in Valsala and Maksyutov (2010).

The second model output used here is taken from the forward simulations of McKinley et al. (2004a). This is also an offline model run with MITgcm circulations and a phosphate dependent ecosystem model. This model comprises of three biogeochemical tracers and they are dissolved inorganic carbon (DIC), phosphate and oxygen. The CO₂ fluxes from this model offer a reasonable comparison with the annual mean air-sea CO₂ fluxes compiled by Takahashi et al. (2009). This data is also used in McKinley et al. (2006). The third model product we used is from Le Quéré et al. (2005) where a

24-component ecosystem is coupled to a state-of-the-art general circulation model (see also Buitenhuis et al., 2006 for details).

3 Results

The three independent products of CO₂ and *p*CO₂ described above are used in this study mainly to seek as robust a conclusion as possible on the climate-carbon connections in the North Pacific. Once a consistent regional and temporal variability of North Pacific CO₂ fluxes are obtained, we perform extended analysis on the optimized estimate of CO₂ flux data of OTTM. We begin our analysis by examining the robustness of our optimized air-sea CO₂ fluxes in the North Pacific in terms of its interannual variability compared to the seasonal cycle. The *p*CO₂ residual errors and error reductions of this optimized data are documented in Valsala and Maksyutov (2010). Here we present results from an extended analysis of the interannual and decadal variability.

The offline model employed in the construction of OTTM fluxes is driven by monthly re-analysis input of ocean currents and other parameters such as temperature and salinity. The only sub-monthly variability present in their model was in the wind speed data used in the calculation of air-sea CO₂ fluxes. However, the model assimilates ship track *p*CO₂ whenever observations are available. Considering the rather coarse resolution (1° × 1°) of the model, it may suffer from representativity errors (RE) while incorporating the high-frequency sampling of ship track data through assimilation. In order to verify the model RE and the signal preserved in the data on seasonal-to-interannual time scales, we performed a signal to noise Ratio (SNR) analysis following a simple method derived from Ballabrera-Poy et al. (2003).

4 Analysis of the Signal to Noise Ratio of air-sea CO₂ fluxes

The SNR analysis of OTTM air-sea CO₂ flux is carried out as follows. The time series of CO₂ flux *c* at each grid point is separated into components of seasonal, *c*^{*s*}, and interannual, *c*^{*a*}, time scales, and noise ε . The seasonal component is calculated by fitting annual and semi-annual harmonics to the total flux *c*. The interannual component, *c*^{*a*}, is found by subtracting *c*^{*s*} from *c*. This, however, will result in a combination of true *c*^{*a*} and ε . A harmonic filtering is then applied to cycles of above the annual period and are subtracted out. The residual is taken as noise, ε . The interannual SNR is calculated as $\sigma_a^2/\sigma_\varepsilon^2$ and total SNR is calculated as $(\sigma_a^2 + \sigma_s^2)/\sigma_\varepsilon^2$; where σ^2 represents the variances of interannual, seasonal and noise components (see Ballabrera-Poy et al. 2003 for further details). The interannual and total SNR are shown in Fig. 1. The interannual SNR is weaker than the seasonal SNR by an order of magnitude. The subarctic and northern

part of the subtropical North Pacific has interannual SNR values below 1 (shaded white). The subtropical and the tropical regions have SNR above 1 and at places values exceeding 3 to 4. The seasonal cycle of the air-sea CO₂ flux also dominates in the North Pacific over the interannual variability. This is consistent with the findings of McKinley et al. (2006) who reported that the counteracting influences of SST, DIC and alkalinity on *p*CO₂ cause a weak *p*CO₂ interannual variability. The interannual variance (see Fig. 1d) is stronger to the east of Japan over the Kuroshio and Oyashio confluence zone. The inverse of this interannual variability is used as a weight to limit the seasonal cycle constraints imposed during assimilation, i.e., the model is allowed to evolve freely in regions where the interannual signals were stronger unless ship track data were available at those locations.

The seasonal variance of air-sea CO₂ fluxes on annual and semi-annual cycles is stronger in the subarctic North Pacific (Fig. 1e). At the northeastern subtropical Pacific, on the other hand, the seasonal variance is weaker. The error variances are mostly located along Kuril and Aleutian Island chains, perhaps indicating that the wind driven coastal upwelling creates high frequency variability (Fig. 1f). It should be also noted that the ship track *p*CO₂ during 1996 to 1998 were sampled through these routes (Zeng et al., 2002). Therefore, the relatively high error variance in this part may be originating from the model's inability to represent high-frequency variability in the *p*CO₂ data during the assimilation.

The SNR analysis suggests that the seasonal cycle in the North Pacific CO₂ fluxes is much stronger than the interannual signal. This is consistent with the findings of McKinley et al. (2006). The interannual variability captured in our estimates should be analyzed in conjunction with the SNR map and should consider only variability in regions where SNR has a value above 1. We will use this as a guidance to assess the interannual variability of the North Pacific CO₂ fluxes retrieved from the subsequent data analysis.

Figure 2 represents the annual mean air-sea CO₂ flux from assimilation as well as from observations of Takahashi et al. (2009). The bottom panel shows the seasonal correlation between assimilation and observations, and they are above 99 % significance level in most parts, with some poor correlation points at grid levels along the island chains of Kuril and the Aleutian, where we observe somewhat higher error variances in the assimilation. Except some differences in seasonal cycle at a few grid points, the overall North Pacific CO₂ flux from assimilation has a remarkably high correlation with the observations. Valsala and Maksyutov (2010; their figures 13 and 14) compared the seasonal as well as interannual variability of air-sea CO₂ flux from this region with data from other sources.

Figure 3 compares the area integrated oceanic CO₂ fluxes among the three data products used here. Note that the three models differ in their approaches of resolving or analyzing the air-sea CO₂ fluxes and inter-model differences are anticipated. The annual mean flux of CO₂ over the North Pacific

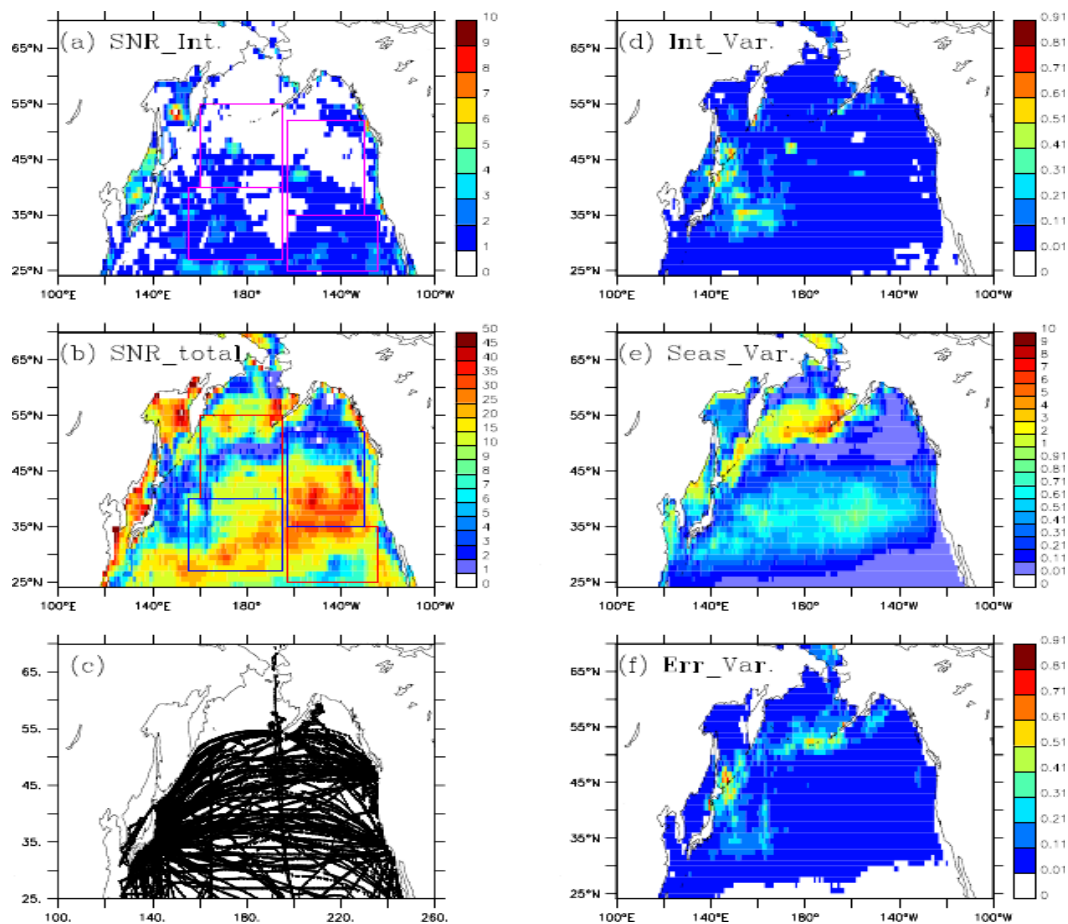


Fig. 1. The Signal to Noise ratio (SNR) of (a) interannual and (b) total air-sea CO₂ flux variability. (c) The total tracks of ship based $p\text{CO}_2$ used in the assimilation between 1996 and 2004. (d) Interannual, (e) seasonal and (f) error variances of air-sea CO₂ fluxes. Units of d, e, and f are in $\times 10^{-14} (\text{mol m}^{-2} \text{seconds}^{-1})^2$. Note that the color bar is different for each figure. SNR below 1 is shaded white. CO₂ flux data from assimilation are used.

domain (100° E–100° W, 20° N–70° N) shows that OTTM, McKinley et al. (2004) and Le Quéré et al. (2005) yields a net oceanic uptake of 0.36, 0.31 and 0.72 PgC, respectively. The seasonal cycles of these three products are fairly in-phase. The interannual anomalies are also quite consistent with each other. Note that we are not focusing here on correlations of area integrated fluxes over the whole domain in order to study the PDO footprints, especially because the PDO signatures in the north Pacific fluxes have more intricate spatial patterns as explored in the following section.

4.1 Correlation between North Pacific CO₂ flux and PDO

The PDO is a decadal mode of climate variability in the North Pacific sector associated with changes in the strength of wintertime Aleutian Low (Trenberth and Hurrell, 1994, also see Schneider et al., 2005 for other contributors to PDO). The accompanying changes in the Ekman flow, surface ocean

mixing and heat fluxes create corresponding anomalies in the ocean. The PDO is defined as the dominant pattern of SST variability in the North Pacific (Mantua et al., 1997). In this study we use the PDO index derived as the leading principal component of North Pacific monthly sea surface temperature variability (poleward of 20° N for the 1900–1993 periods) and obtained from <http://jisao.washington.edu/pdo/>. The PDO goes through warm and cool phases with each phase typically lasting about 20–30 years. The causes of this phase swings are currently unknown and the mechanisms or the independence of PDO as a climate mode are also debated (e.g., Rodgers et al., 2004; Newman et al., 2003). The recent decades have seen a cool phase starting around 1945 switching to a warm phase in 1977. The warm phase continued until late 2008 with some short cold spells in the PDO index (see <http://jisao.washington.edu/pdo/> for an up-to-date report). The warm epochs of PDO are associated with enhanced coastal ocean biological production in the Alaska sector and with inhibited productivity off the west coast of the

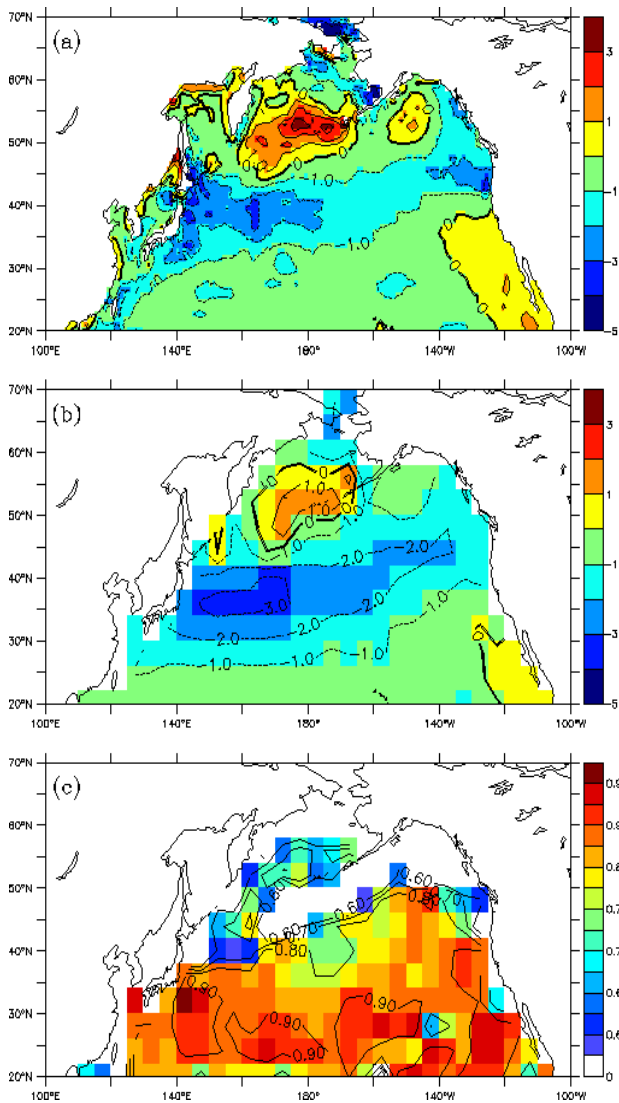


Fig. 2. Annual mean net air-to-sea CO₂ flux (negative represents CO₂ flux from atmosphere to ocean and vice versa) from the North Pacific from (a) the assimilation and (b) Takahashi et al. (2009). Units are in mol m⁻² yr⁻¹. (c) Seasonal correlation coefficients between assimilation and Takahashi et al. (2009) are shown only for those correlations above the 5 % level.

United States, while cold PDO episodes tend to produce the opposite north-south pattern of marine ecosystem productivity (Mantua et al., 1997).

In order to identify the spatial patterns of the North Pacific CO₂ flux variability with respect to PDO, we start with a simple correlation analysis. The CO₂ fluxes are deseasonalized and detrended before calculating the correlations. Figure 4 illustrates the point-to-point correlation between monthly air-sea CO₂ flux anomalies and PDO index for three flux products, viz., (left) OTTM and forward models of (middle) McKinley et al. (2004a) and (right) Le Quéré et al. (2005). The correlations coefficients are estimated from 300 monthly

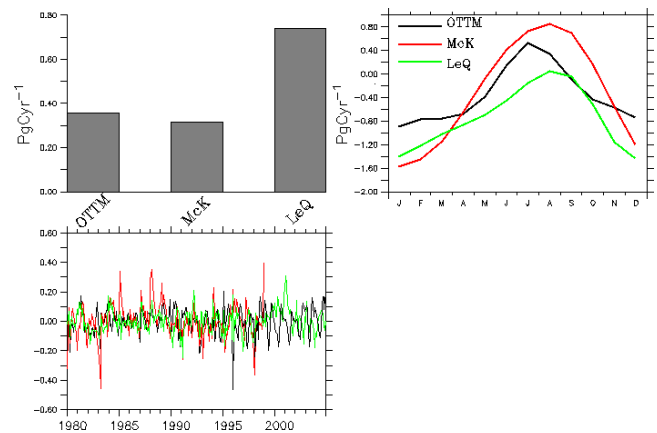


Fig. 3. The area integrated net air-to-sea CO₂ fluxes over north Pacific (100° E–100° W, 20° N–70° N) shown for annual mean (top-left), seasonal cycle (top-right) and interannual anomalies (bottom) from three data product. The units are in PgCyr⁻¹. Positive (negative) value means a source (sink) of CO₂ for the atmosphere except for the bar-diagram where positive means a net sink.

values between 1980 and 2004 in the OTTM data set and Le Quéré et al. (2005) and the corresponding monthly PDO index. In the case of McKinley et al. (2004a), only 240 months are used from 1980 to 1999. All the correlations shaded are significant using a 90 % confidence interval in a two-tailed *t*-test. A careful examination of the correlation patterns suggests that PDO organizes regional responses in the air-sea CO₂ flux anomalies of the North Pacific. Considering both the clustering of correlations and the SNR of the interannual signal (see Fig. 1), we categorized four poles of positive and negative correlations. The positive correlation poles are located in the northwest and southeast part of the domain. Other two poles of negative correlations are oriented in the northeast and southwest direction of the domain. It can be seen from Fig. 1a that the interannual SNRs are reasonably large in the southern poles, whereas they are relatively weak but statistically significant in the northern poles. We discarded the correlations on the subarctic North Pacific from the poles because their interannual SNR is below 1. Note that the trend of CO₂ fluxes which has been removed prior to the correlation analysis has no such regional patterns (figures not shown).

A similar analysis of the other two flux estimates (column 2 and 3 of Fig. 4) shows that such regional structures are quite consistent among the three CO₂ products. However slight re-orientation of boxes is required when we move from one data product to another, which is not unexpected because they are generated by entirely different sets of models with additional differences in resolutions and surface forcing.

Looking at the clustering of correlations in individual poles, we defined an index of CO₂ flux in response to PDO (hereafter CO₂g_PDO) as the sum of area integrated CO₂ anomalies from two “red” boxes minus the corresponding

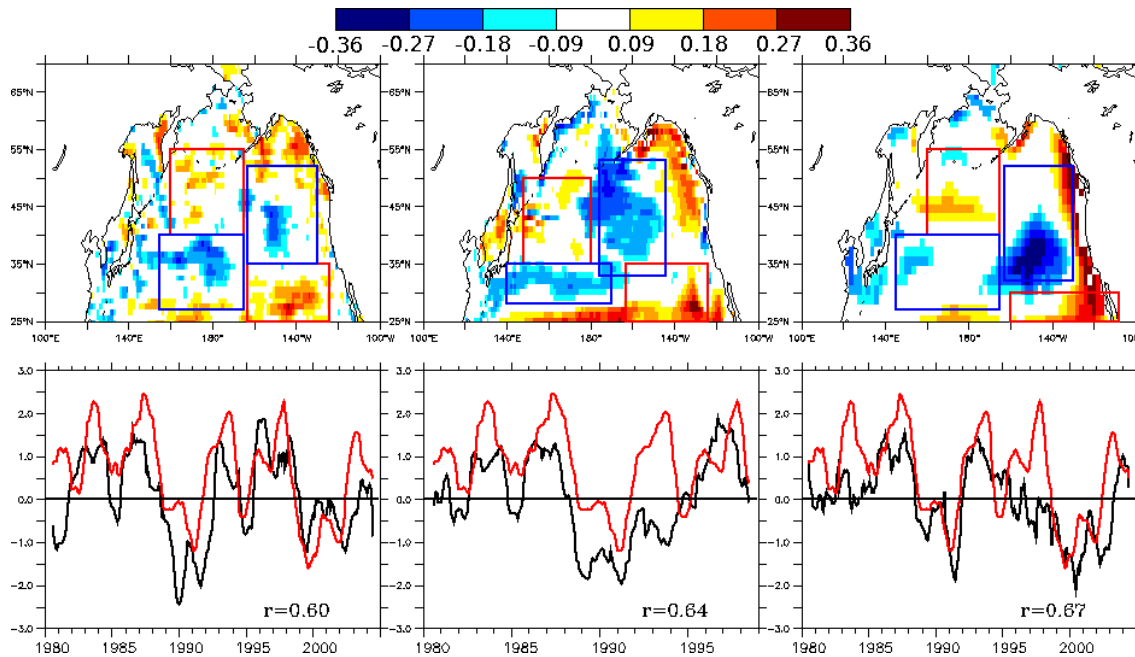


Fig. 4. (Top panels): Correlation coefficients (r) between the interannual variability of net air-to-sea CO₂ flux (computed as monthly anomalies of CO₂ flux) and the PDO index from three data products; (left) assimilation, (middle) McKinley et al., 2004 and (right) Le Quéré et al., 2005. Sign convention of CO₂ flux is same as in Fig. 2. Significant correlations at 90% confidence intervals are shaded. (Bottom panels): CO₂ flux index corresponding to PDO from the three data products (black lines) and the PDO index (red lines). See text for the calculation of CO₂ flux indices. All lines are smoothed by 12-month running mean and normalized by respective standard deviations to fit into a common y-axis. The “ r ” of bottom panels is significant at a 95 % confidence interval.

sum over the two “blue” boxes (see Fig. 4 for boxes). The index is shown in the bottom panel of Fig. 4 for each product as the black line. The PDO index is overlaid as a red line. Both lines are smoothed with a 12-month running mean (all time-series shown hereinafter are smoothed by a 12-month running mean for consistency). The CO₂_g-PDO and PDO correlate with each other (using a 95 % confidence interval), especially because the regions for calculating CO₂_g-PDO are chosen from areas where the correlations with PDO are significantly high. Therefore the interannual-to-decadal CO₂ flux anomalies in the North Pacific are clearly and fairly intimately related to PDO in the region represented by the four poles shown in these figures.

Air-sea CO₂ flux is driven by the difference in p CO₂ between the ocean and the atmosphere as well as the piston velocity which is usually parameterized with wind speeds (e.g., Wanninkhof, 1992). In order to see what controls the CO₂ flux variability linked to PDO, we repeated the correlation analysis with the optimized OTTM p CO₂. The results are shown in Fig. 5. It can be seen that similar regional structures of correlations between p CO₂ and PDO exist as in the case of CO₂ fluxes. Therefore, the air-sea CO₂ flux anomalies linked to PDO as seen in the previous analysis are mainly driven by the p CO₂ anomalies. The index representing the p CO₂-PDO also correlates with PDO index significantly using a 95 %

confidence interval. Since seawater p CO₂ is controlled by solubility and biological pumps, the biological pump relies to a large extent on the vertical supply of nutrients (horizontal advection can also be important), we expect that ocean dynamics, i.e., thermocline movements and mixed layer entrainment are crucial. The solubility pump on the other hand is more closely related to the thermodynamics, i.e., SST variability. An additional characteristic of this region is that the so-called transition zone chlorophyll front (TZCF) traverses this entire domain and demarcates the subtropical-subpolar boundary with a clear and significant impact on not only the dynamics and the thermodynamics of our domain but also the ecosystem and the biogeochemistry of all the poles being studied here (Polovina et al., 2001). Detailed analysis of the interactions between the TZCF, PDO, and the correlations being discussed here is beyond the scope of the present study.

4.2 Interannual and Interdecadal relations between CO₂ fluxes and PDO

There is considerable uncertainty about whether the PDO is truly independent of the leading mode of tropical variability, i.e., ENSO (Rodgers et al., 2004; Newman et al., 2003). The spatial patterns of interannual SST variability in the Pacific Ocean show a pronounced maximum in the tropical

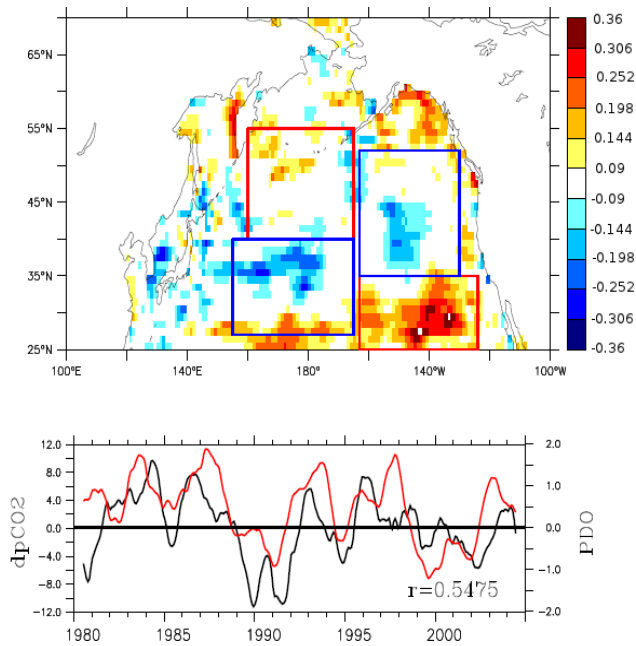


Fig. 5. (Top): Correlation coefficients between the interannual variability of $\delta p\text{CO}_2$ and the PDO index (negative $\delta p\text{CO}_2$ means atmospheric $p\text{CO}_2$ exceeds that of the ocean). Correlations significant at 90 % confidence interval are shaded. (Bottom): $\delta p\text{CO}_2$ index corresponding to PDO (black line) and PDO index (red line). $\delta p\text{CO}_2$ data from assimilation are used. Time series are smoothed by 12-months running mean. Correlation is significant (using a 95 % confidence interval).

east Pacific and weaker center of opposite sign in the central North Pacific. While on decadal timescales, the relative strength of these centers is reversed (Zhang et al., 1997). The simultaneous correlations of ENSO index and PDO are relatively weak especially during winter months (Mantua et al., 1997).

It is evident from the CO₂g_PDO index shown in Fig. 4 that the index has both a low-frequency (i.e., a decadal time scale) and a high-frequency (interannual) component. Therefore it is reasonable to expect that the individual correlations between decadal and interannual variability of CO₂ flux are linked to PDO. Here “decadal” is not intended to represent a 20–30 year cycle at which the PDO typically switches between cold and warm phases. But the focus is on periods longer than ENSO and in the range of 10–15 years.

In order to show separate correlations of CO₂g_PDO index at these two time scales, we isolated the decadal component of CO₂ flux variability using the harmonic filter analysis. The variability of 6.5 years and above was filtered out from the interannual anomalies of CO₂ flux and correlations with correspondingly filtered PDO index are computed. Figure 6 illustrates that the correlation found both at decadal and on interannual time-scales are almost identical albeit with some differences in the intra-box correlation features. Here

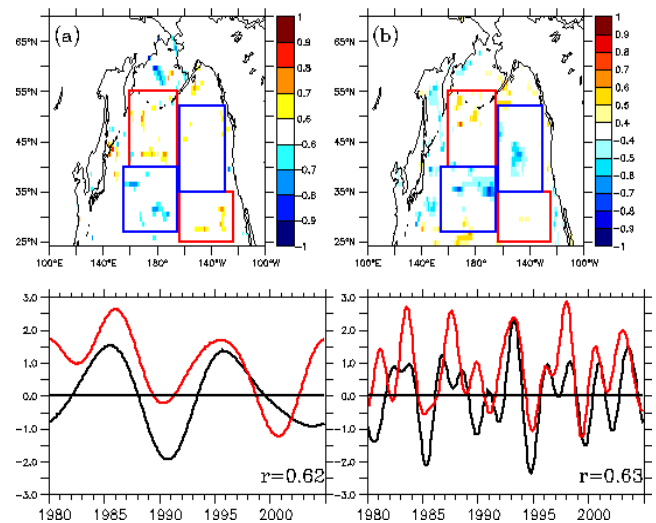


Fig. 6. Same as Fig. 4 left column but for separated components of (left) >6.5 year cycles and (right) <6.5 year cycles of net air-to-sea CO₂ flux anomalies and PDO. Correlations significant at 90 % confidence interval are shaded. CO₂ flux data from assimilation are used.

we note that separating the cycles of 6.5 years and above out of 25 years of data restricts the degrees of freedom of the signal to be below 4. Therefore the significant correlations above the 10 % level (or significant using a 90 % confidence interval) leave only few visible points in each of the poles considered here. For instance, the northwestern pole is consistent between the two cases (see Fig. 6a and b). However, there are differences in correlations over the northeast pole between the interannual and decadal time-scales. The southwest pole shows a stronger decadal than interannual signal. The bottom panels show the CO₂g_PDO and PDO indices at both decadal and interannual time-scales. Both correlate at significantly at a 90 % confidence interval. This analysis allows us to conclude that the correlations between CO₂ fluxes in the North Pacific and the climate drivers are significant both at low and high frequencies.

It is a general practice to discuss the North Pacific variability as a seasonal average variability only during the winter months because of the weak correlations between the winter time PDO and ENSO (Mantua et al., 1997). We calculated the correlations of winter PDO with corresponding winter CO₂ flux anomalies. The months from November to March are used to represent the winter-PDO, and the CO₂ flux anomalies of corresponding months are also averaged prior to computing the correlations. Similarly summer months of June and July are used for summer-PDO and CO₂ flux correlations. Figure 7 shows that the winter-PDO produces a quadru-pole structure in the correlation with the same polarity as was seen in the previous sections. On the other hand, during summer months this quadru-pole polarity is lost and the North Pacific CO₂ flux is largely negatively correlated

with the summer-PDO with some positive correlation only in the southeast pole. This analysis shows that the winter time PDO is essentially responsible for producing a quadru-pole structure in the North Pacific CO₂ fluxes with positive polarity in the northwest and the southeast poles and with opposite polarity in the other two poles. This again confirms that such a distribution of the North Pacific air-sea CO₂ fluxes is driven by the PDO because the signal is stronger during winter months when the “grip” of ENSO on PDO is weaker. The subpolar-subtropical-tropical interactions have seasonal variations which affect the seasonal vulnerability of our study region to climate modes (see for ex., Vimont, 2005). The seasonal aspects of this are also important since the subtropical anticyclone itself undergoes a significant weakening during the winter and the subpolar low expands to reach into the tropics (Nigam and Chan, 2009). The dynamical and thermodynamical responses of these changes on CO₂-flux variability will need further detailed analysis which is beyond the scope of this study.

In order to provide additional support for individual effects of PDO and ENSO on the correlations with CO₂ fluxes, we performed a “partial correlation” analysis. In case of a set of three variables which show mutual correlations, the partial correlation analysis attempts to remove the effect of one component over the other two (Ashok et al., 2007). Figure 8 shows the correlations between monthly PDO index and CO₂ flux anomalies after removing the effect of ENSO through partial correlation analysis. The quadru-pole structure with diagonal polarities is still maintained in this case confirming the PDO as the dominant driver of the correlation features in the North Pacific air-sea CO₂ fluxes. Again, to untangle the dynamic and thermodynamic forcing components of the CO₂ variability, the persistence of PDO and its impacts on wind-speeds and wind-stress curls have to be analyzed together with ENSO impacts on the same. In hindsight, it is not surprising that PDO dominates the region, since ENSO is most directly teleconnected to the Aleutian low which occupies the northwest corner of our domain, whereas PDO signature affects all four poles and persists over decadal time-scales. We use combined EOF analysis to extract some clues into the dynamic and thermodynamic contributions to CO₂ variability in the study domain.

4.3 Component analysis of CO₂ fluxes with ocean-atmosphere variability

Although the correlation analysis presented above identifies the spatial and temporal structures of the North Pacific CO₂ flux variability with respect to PDO, it does not, by itself, offer any mechanistic insights. We carried out a component analysis of *p*CO₂ in terms of SST, DIC, Alkalinity and Salinity and performed the correlations with each of them. These components are obtained by a method similar to that described in McKinley et al. (2006). Our results are similar to the findings of McKinley et al. (2006) in that the partial

changes of *p*CO₂ due to SST, DIC and Alkalinity are similar in magnitude and opposite in phase. Thus the net change in *p*CO₂ is the sum of the partial changes of these factors, and the residual of the sum is the interannual variability. In our study, the correlation analysis only organizes this residual interannual variability in a certain regional pattern. Considering the robustness of correlation patterns between the three data products examined here, it seems reasonable to assume that their existence is not purely by chance.

In this section, we examine the combined variability of air-sea CO₂ fluxes in terms of a few oceanic and atmospheric variables in order to see their covariability with PDO. We employed a combined empirical orthogonal function (CEOF) analysis between these pre-selected variables. CEOs capture the joint variability of two variables in space and time. If such variability exists in the case of North Pacific CO₂ fluxes and if they correlate with PDO, it should provide a basis for the existence of the spatial structure and point to the mechanism responsible for the structure of interannual CO₂ flux variability.

We begin the analysis by calculating the CEOs between the anomalies of CO₂ fluxes and SST over the domain under consideration. The CEOs of detrended, de-seasonalized CO₂ flux and SST anomalies were calculated. The data are passed through a 12-month running mean before computing the CEOF (and therefore, the time-series hereinafter are not applied the 12-month running mean). The SST anomaly was taken from Simple Ocean Data Assimilation prepared by Carton and Giese (2008). The top-panel of Figure 9 shows the spatial patterns from the CEOF-1 of CO₂ flux and SST anomalies. And the bottom panel shows the principle components (PC) of the dominant mode. The red line in the bottom panel shows the PDO index. All the spatial patterns (i.e., CEOs) are multiplied with standard deviations of respective variables. Therefore they have meaningful units. All PCs are normalized with respective standard deviations in order to non-dimensionalize them.

The CEOF extracts the response of CO₂ related to SST and their PC-1 shows a clear correlation with PDO (above the 5 % level). Therefore, the dominant mode of SST variability in the North Pacific does have an influence on defining the dominant mode of variability in the CO₂ flux. This is clear evidence that the North Pacific CO₂ fluxes do respond to PDO. The CEOF-1 of SST combined with CO₂ flux shows a typical PDO signature in SST during a warm phase as shown in Mantua et al. (1997). The corresponding CO₂ flux responses show a sink in the subtropical gyre where the SST anomalies are found to be negative. This shows a direct relation between *p*CO₂ and SSTs, i.e., a reduced *p*CO₂ during a cold SST anomaly. In the northern subtropical to sub-arctic North Pacific, the CO₂ flux maybe expected to show a positive anomaly in response to the warm anomaly in SST. However, there are negative anomalies of CO₂ flux at few spots corresponding to positive SST anomalies. This is likely a combination of the noise in the model (SNR in this region

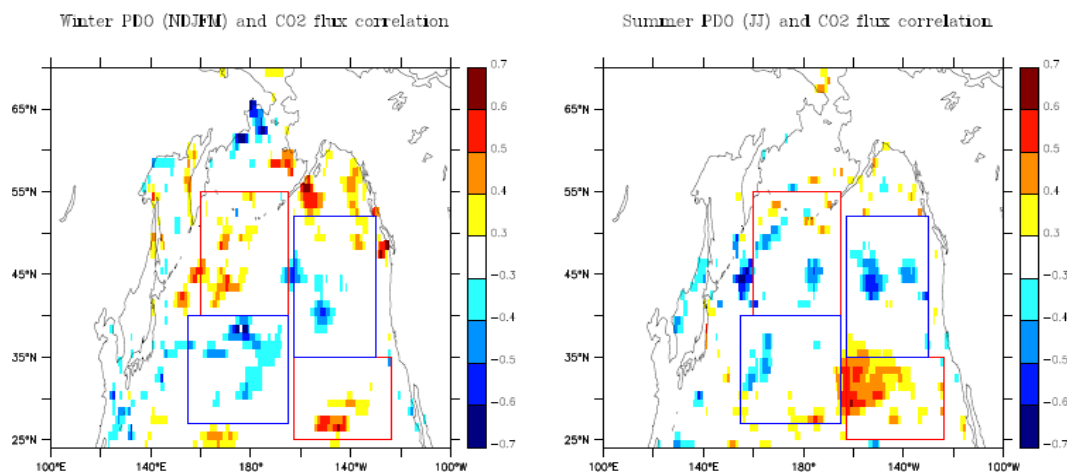


Fig. 7. Same as Fig. 4 left column but correlations are computed for (left) winter month and (right) summer month net air-to-sea CO₂ flux anomalies with corresponding PDO index. Significant correlations above the 5 % level are shaded.

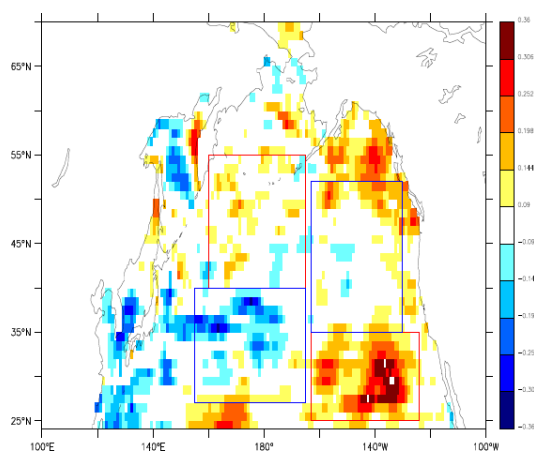


Fig. 8. Partial correlation between net air-to-sea CO₂ flux anomalies and PDO after removing the correlations between CO₂ flux anomalies and ENSO. CO₂ flux data from assimilation are used. Correlations significant at 90 % confidence interval are shaded.

is significantly low; see Fig. 1) and the dynamic component of the CO₂ flux variability (see discussion below). In fact the Aleutian low and the Kuroshio add significant dynamic component to the flux variability. The variance explained by CEOF-1 is 18 %.

We also calculated the CEOF of CO₂ flux and wind stress anomalies. We choose the wind stress in this analysis because it offers a squared wind relation with the CO₂ flux, which corresponds to the squared wind speed and variance used in the CO₂ exchange calculation. The results are shown in Fig. 10. The top-panel shows the CEOF-1 of CO₂ flux and wind stresses, which is very similar to the CEOF-1 of CO₂ flux and SST (cf. Fig. 9). Wind stresses (vectors) show the dominant mode of wind pattern corresponding to the warm

phase of PDO (Mantua et al., 1997). The middle panel shows the CEOF-1 of SST and wind vectors from CEOF with CO₂. This panel shows a clear PDO type SST-wind relationship as can be expected because of the dominance of PDO forcing. The bottom-panel shows the PC-1 of CO₂ with wind stresses (black line) and PDO index (red line). The variance explained is 20 %. The PC shows that the North Pacific CO₂ sink strengthens when the zonal winds associated with the PDO are stronger. This can be seen from the CEOF-1 pattern of CO₂ and wind stress components in the top-panel of Fig. 10. Both PCs (Figs. 9 and 10) and PDO index significantly correlate with each other (using a 95 % confidence interval).

The CEOF analysis was also done between CO₂ fluxes and sea surface height (SSH) anomalies. The concomitant analysis of CEOFs of CO₂ and SSH as well as CO₂ and SST provides insights into the dominant mechanisms of CO₂ interannual variability in terms of dynamic and thermodynamic contributions. Figure 11 shows CEOF analysis of CO₂ and SSH anomalies. The top-panel of the figure shows that the interannual variability of CO₂ has a similar structure in SSH as that found in SST and wind stresses. This co-variability of CO₂ fluxes with SSH, SST and wind anomalies show their strong mutual coupling through dynamics and thermodynamics. For example, the subtropical gyre shows a CO₂ sink in the CEOFs of CO₂ with SST and SSH. This leads to the conclusion that there is a dominant thermodynamic control on CO₂ fluxes in the subtropical gyre. For example, a cold SST anomaly leads to a sink of CO₂ through enhanced solubility. On the other hand, the shoaling of thermocline in the subtropical gyre and the increase in surface DIC has no net influence on CO₂ fluxes since it is counteracted by increased solubility and a relatively small increase in CO₂ flux. The role of the dynamics is thus muted by the thermodynamics. It is worth mentioning that the seasonal cycle of

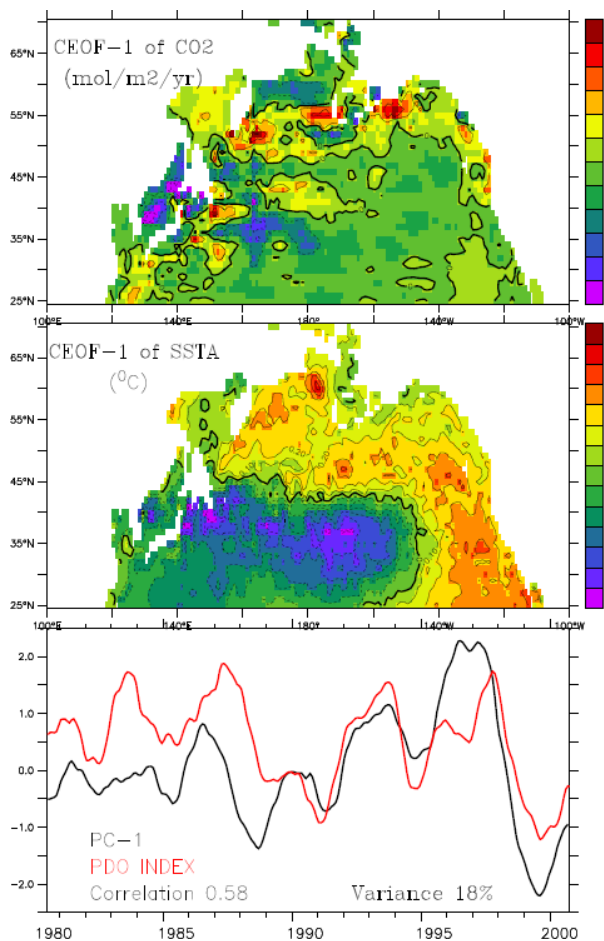


Fig. 9. (top) The spatial pattern of CEOF-1 for net air-to-sea CO₂ flux anomalies (negative represents CO₂ flux from atmosphere to ocean and vice versa) and (middle) that for SST anomalies. (bottom) PC-1 (black-line) and PDO (redline). Time-series are significantly correlated above the 5% level.

CO₂ fluxes in the North Pacific is nearly an order of magnitude larger than the corresponding interannual variability. The seasonal cycle of CO₂ flux is strongly influenced by the thermodynamics of the mixed layer, and slight changes in the seasonality from year to year drive interannual variability of CO₂ fluxes in the subtropical gyre of the North Pacific.

The thermodynamic control on CO₂ fluxes, however, appears to be weaker in the subarctic North Pacific. This is elicited by examining the top-panels of Figs. 9, 10, and 11. These three panels show that there are marked differences in the CO₂ flux variability explained by SST, wind and SSH. In order to see what causes the regional clustering of correlations of CO₂ fluxes with PDO (see Sect. 3.1), we carried out the combined CEOF analysis of CO₂ flux, SST and SSH together and results are shown in Fig. 12. The combined variability of SST and SSH (or can be rightfully interpreted as covariability of thermodynamics and dynamics) causes a

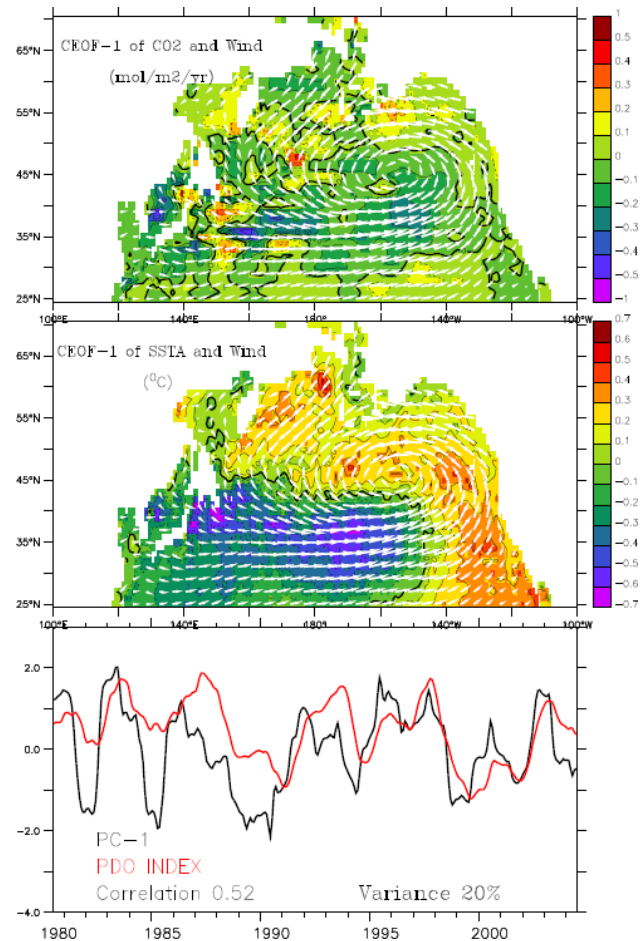


Fig. 10. Same as Fig. 9, but for CEOFs of CO₂ flux and wind stress anomalies. The middle panel is same as the middle panel of Fig. 9, but CEOF-1 wind stress vectors overlaid.

tentative quadru-pole shape in the CEOF of CO₂ flux (top-panel of Fig. 12). For the purpose of comparison, the regional clustering of correlations as explored in Sect. 3.1 is repeated in the middle panel of the figure. This panel suggests that the combined influence of dynamics and thermodynamics can cause such regional homogeneity of CO₂ flux variability in response to the PDO. The bottom panel of the figure shows the PC-1 of CEOF, the CO₂g_PDO and PDO indexes. They significantly correlate with each other (using a 95% confidence interval; correlations range between 0.54 and 0.62).

The spatial and temporal correlations between CEOF-2 of CO₂ and other variables described above in the CEOF analysis were also similar and significant. This is consistent with the findings of McKinley et al. (2006) in that the first two EOFs show significant correlations with PDO. However the relation and independence of EOF-1 and 2 type inter-annual variability between PDO and ENSO have been discussed in several previous studies and a clear conclusion is

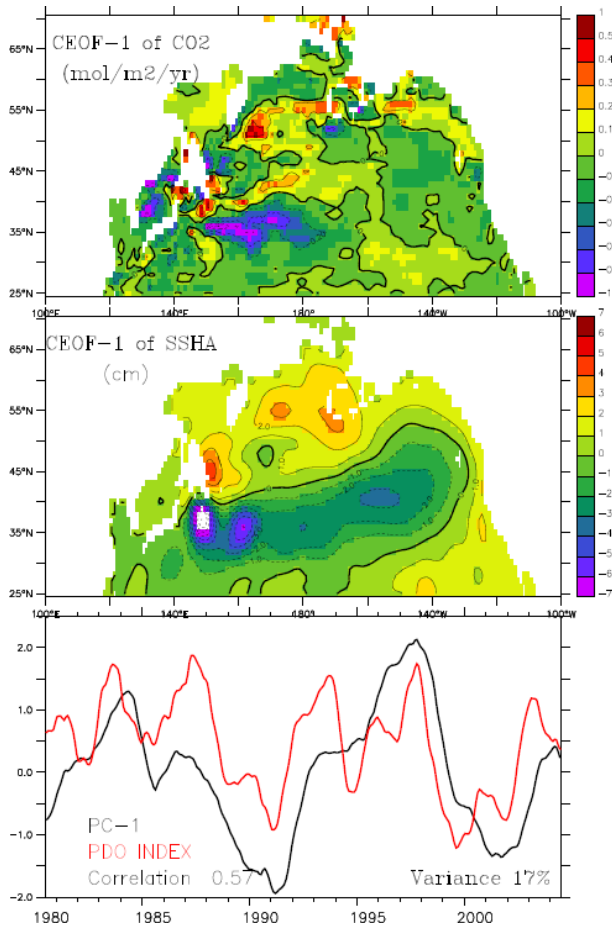


Fig. 11. Same as Fig. 9, but for CEOFs of CO₂ flux and SSH anomalies.

not available yet (Lorenzo et al., 2008; Latif and Barnett, 1996). Therefore, we restrict our analysis to the first modes of EOFs.

5 Discussion and conclusion

Several features of the interannual variability of air-sea CO₂ flux linked to PDO are isolated in this study. The results lead to interesting insights in terms of assessing the trends in the surface ocean *p*CO₂. Our analysis puts forward a recommendation that we should take into account the natural variability while assessing the secular trends in the *p*CO₂ of the North Pacific, especially when they are based upon short term observations. Our analysis suggests that such trends could be a manifestations of the larger natural interannual to decadal variability. Takahashi et al. (2006) examined the 30-years of trend from sparse observations available. They noted that except for the Bering and Okhotsk Seas the *p*CO₂ trends are positive. However our analysis indicates a much finer regional characterizations of decadal variability in the North Pacific.

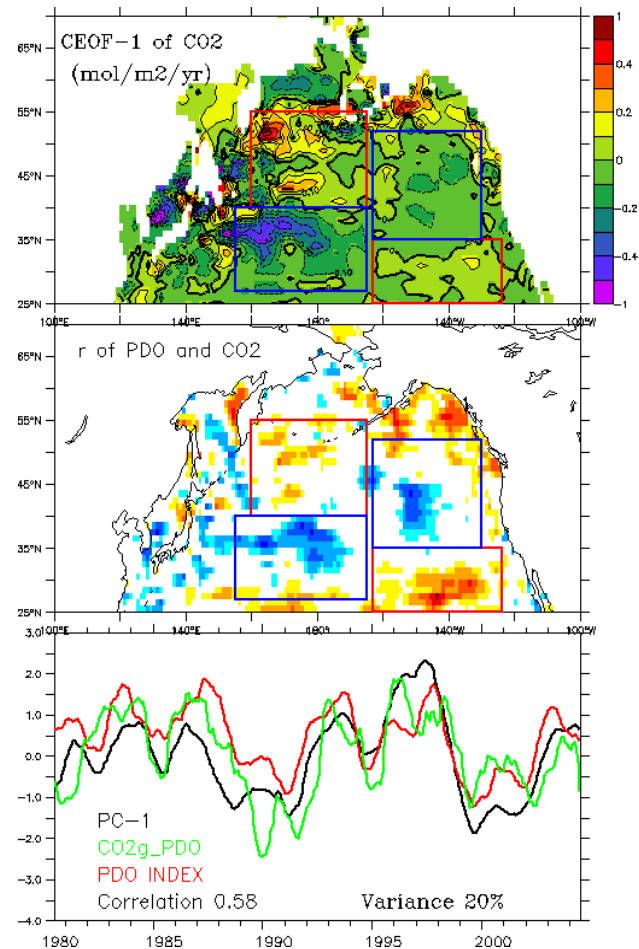


Fig. 12. (top) Spatial pattern of CO₂ flux from CEOF of CO₂ flux with SST and SSH. (middle) Same as top-left panel of Fig. 4. (bottom) PC-1, CO₂g_PDO and PDO index (see Fig. 4 caption for more details). The correlation (0.58) shown is between PC-1 and PDO index.

Although the correlative as well as CEOF analyses identified a spatial structure of CO₂ flux variability with the PDO, the magnitude of the anomalies is relatively small. This can be expected in the case of North Pacific CO₂ fluxes because it has weak interannual anomalies. We regressed the PDO index against CO₂ fluxes over the four-poles depicted in the above analysis and found that the net variability is a sink of 0.015 PgCyr⁻¹ (Fig. 13). In the figure, the regressed anomalies are shown only where the SNRs of interannual variability are above one. The regressions are shown only for those anomalies whose amplitude is above 1-sigma. It is interesting that a positive PDO causes a net air to sea flux in the North Pacific, but we note that this value is derived only over a portion of the region of North Pacific which satisfies the SNR criteria. Therefore, the accuracy of this estimation may depend upon the model's capability to capture the SNR adequately. The annual mean sink of CO₂ in the domain under

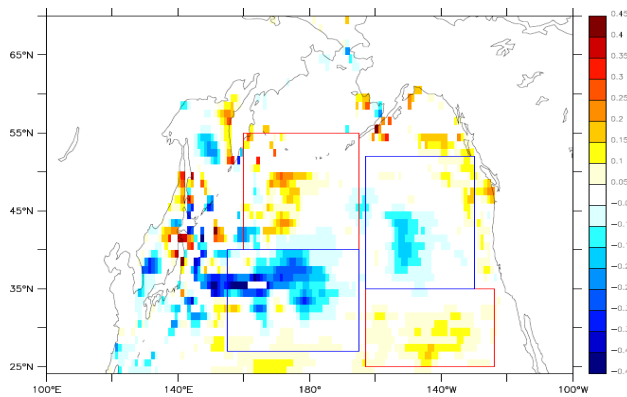


Fig. 13. Regressed net air-to-sea CO₂ flux anomalies (negative represents CO₂ flux from atmosphere to ocean and vice versa, mol m⁻²yr⁻¹) over PDO.

consideration is, however, nearly 0.35 PgCyr⁻¹. The internal variability and the inability to extract the internal variability from limited data appear to be a major impediment to robust conclusions about the source/sink variability in the domain. Thus, estimating the SNR as best as we can becomes critical.

The analysis presented here used three independent CO₂ products and attempted to extract the most robust features in the regional responses of air-sea CO₂ fluxes in the North Pacific to climate anomalies. In addition to the surface fluxes, we also extended the analysis to the ocean interior in order to retrieve deep structures of interannual variability as visible in the model outputs of DIC. Our analysis revealed that the subsurface DIC also responds to the thermocline movements induced by the PDO forcing. For example, Fig. 14 depicts the correlation coefficients between model DIC and PDO index (top-panel) at the surface level and (middle-panel) at a 100 m depth level. The overlaid contours are that of CEOF-1 of SST and CO₂ flux. The cold SST anomaly reflects an increase in DIC both in the surface as well as at 100 m depth, which indicates a shoaling of the thermocline and subsequent increase in DIC (see also McKinley et al., 2006). However, it is likely that such an increase in DIC is ineffective in driving CO₂ flux responses which appear to be mostly controlled by the SST cooling, especially in the subtropical gyre of the North Pacific. This is confirmed by the CO₂ flux anomalies in the subtropical gyre which show a sink (top-panels; Figs. 9, 10 and 11) indicating an active response of CO₂ fluxes to the cold SST anomalies associated with the PDO (middle-panel; Figs. 9 and 11). This leads to the conclusion that the thermodynamics (i.e., SST and CO₂ flux relationships) plays a dominant role in the subtropical Pacific.

Figure 14 also shows a vertical propagation of the PDO signal. The signal is illustrated as a vertical section of correlation coefficients between DIC and PDO, averaged zonally over 140° E to 140° W. The correlations extend to the

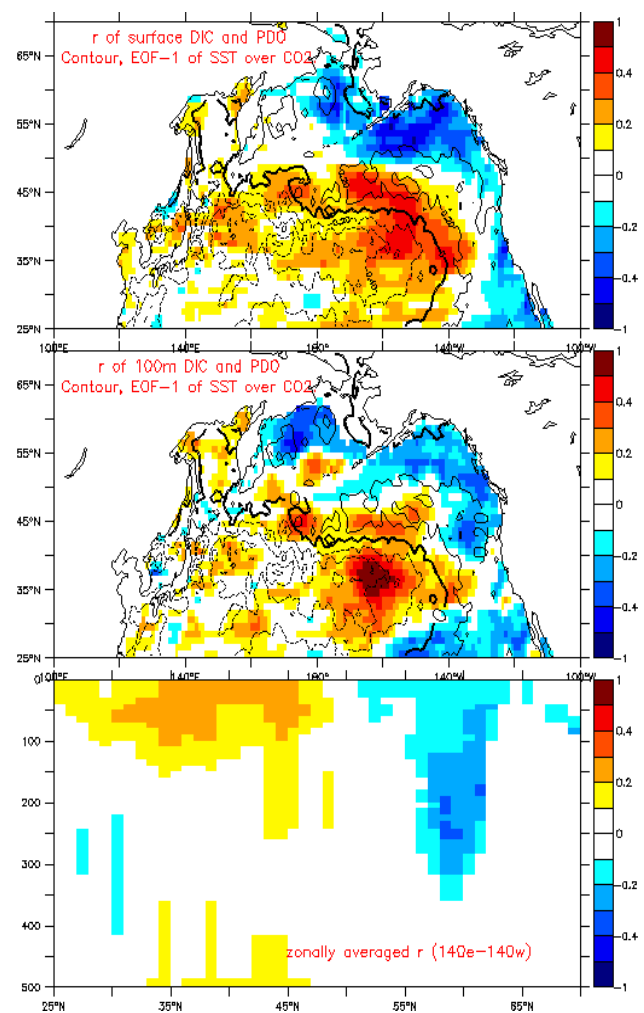


Fig. 14. Correlations between DIC and PDO shown for the (top-panel) surface and for (middle-panel) 100 m depth level. Spatial pattern of SST from CEOF-1 of SST and CO₂ flux is overlaid as contours. Bottom panel shows the vertical section of correlations averaged over a zonal dimension of 140° E to 140° W. Correlations significant at 90 % confidence interval are shaded.

thermocline in the subtropical region (to ~100 m) which is within the reach of seasonal mixed layer, whereas they extend to a depth greater than 300 m in the subarctic region. The seasonal amplitude of mixed layer depth (winter maximum minus summer minimum) in the subtropical region is ~100 m (with annual mean mixed layer depth of 110 m) whereas in the subarctic region it is ~50 m (with annual mean mixed layer depth of 90 m). The extent of vertical propagation of PDO signal in the subtropical region shows that the seasonal cycle of vertical mixing carries the PDO induced surface changes to the thermocline, again indicating that the thermodynamic cycle could be the dominant mechanism of air-sea CO₂ fluxes in that region. In contrast, the vertical propagation of the PDO signal in the subarctic is

much deeper even with the shallow seasonal amplitude of the mixed layer depth of only 50m. Therefore, one may assume that the role of dynamical changes in thermocline depths may be significant in this region. This is consistent with the EOFs between CO₂ and SSH as well as between CO₂ and SST in the subarctic region. The SSH induced deepening of the thermocline and negative CO₂ flux anomalies should be noted especially in the eastern subarctic gyre (see Fig. 11).

In our analysis, as well as in McKinley et al. (2006) it is reflected that the individual components that control the surface ocean pCO₂ in the North Pacific respond to PDO with significant amplitudes, whereas their combined effects make a net contribution which is feeble in amplitude, and scattered in space. Despite this general agreement, our study suggests that, within the scattered spatial correlations of CO₂ flux anomalies with PDO, there seem to be regional clustering of positive and negative correlations, and we propose that they are organized into four distinct regional poles. This hypothesis was tested with three different CO₂ products, and a general conclusion is reached. The implication of our results is that the assessment of pCO₂ trends in terms of surface ocean pCO₂ should consider the natural variability and its regional patterns.

Certain caveats with the present analysis must be borne in mind though. The conclusion drawn here are mainly based on analyzing a limited record of CO₂ flux data. 25-years of data perhaps are not resolving the much longer PDO cycles completely. However because of the limitation in the availability of high quality air-sea CO₂ flux data on multi-decadal scales we restrict our analysis to the given period of time. The three model data products are compared here and they revealed a consistent result and that provides the confidence that such relations of PDO and CO₂ fluxes can be robust.

The conclusions of this study are restated here. (1) The North Pacific air-sea CO₂ fluxes show significant regional correlations with the PDO and they are oriented along two positive poles in the northwest-southeast directions and two negative poles in the northeast-southwest direction. (2) The combined and individual effects of ENSO and PDO on the regional clustering of correlations were identified and it is shown that PDO is the dominant cause for such regional correlations. (3) The combined EOF analyses were carried out between CO₂ fluxes and few key variables of air-sea interactions and it was found that in the subtropical North Pacific, the air-sea CO₂ fluxes are generally controlled by the thermodynamics (i.e., vertical mixing, seasonal cycle of SST and CO₂ fluxes), whereas, in the subarctic North Pacific, there could be a dominance of dynamically induced controls on the CO₂ fluxes (i.e., wind induced thermocline heaving, surface DIC convergence and CO₂ fluxes). However, we note that the last point is only suggested by our study and it requires more model simulations and diagnostics as well as ecosystem assessments in order to fully reveal the controls of thermodynamics and dynamics in the interannual variability of air-sea CO₂ fluxes in the North Pacific. That is left as a future study

and will be reported elsewhere. To the extent that climate change is expected to manifest into changes in ENSO and PDO, the climatic impacts on the carbon cycle are also expected to occur through these dynamic-thermodynamic processes in addition to ecosystem responses. Our study will hopefully provide a framework to assess the response of the air-sea exchanges of CO₂ and the oceanic carbon cycle to climate change.

Acknowledgements. This work was carried out as part of the GOSAT carbon cycle research project at CGER, NIES. Computational resources were provided by the supercomputer facility at NIES. MT acknowledges the use of the High Performance Computing Cluster supported by the Research Computing Service at the University of East Anglia, Norwich, UK. MT, SN and YN were kindly supported by Global Environmental Research Account for National Institutes from Ministry of Environment, Japan. RM gratefully acknowledges the generous support by the Divecha Climate Center and the hospitality of CAOS at IISc, Bangalore.

Edited by: F. Joos

References

- Ashok, K., Nakamura, H., and Yamagata, T.: Impacts of ENSO on the Southern hemisphere storm-track activity during Austral winter, *J. Climate*, 20, 3147–3163, 2007.
- Baker, D. F., Doney, S. C., and Schimel, D. S.: Variational data assimilation for atmospheric CO₂, *Tellus*, 58B, 359–365, 2006.
- Ballabrera-Poy, J., Murtugudde, R., and Christian, J. R.: Signal-to-noise ratio of observed monthly tropical ocean color, *Geophys. Res. Lett.*, 30(12), 1645, doi:10.1029/2003GL016995, 2003.
- Buitenhuis, E., Le Quéré, C., Aumont, O., Beaugrand, G., Bunker, A., Hirst, A., Ikeda, T., O'Brien, T., Piontkovski, S., and Straile, D.: Biogeochemical fluxes through mesozooplankton, *Global Biogeochem. Cycles*, 20, GB2003, doi:10.1029/2005GB002511, 2006.
- Carton, J. A. and Giese, B.: A reanalysis of ocean climate using Simple Ocean Data Assimilation (SODA), *Mon. Wea. Rev.*, 136, 2999–3017, 2008.
- Chavez, F. P., Pennington, T. J., Castro, C. G., Ryan, J., Michisaki, R. P., Schlining, B., Walz, P., Buck, K., McFadyen, A., and Collins, C. A.: Biological and chemical consequences of the 1997–1998 El Niño in central California waters, *Progr. Oceanogr.*, 54, 205–232, 2002.
- Di Lorenzo, E., Schneider, N., Cobb, K. M., Franks, P. J. S., Chhak, K., Miller, A. J., McWilliams, J. C., Bograd, S. J., Arango, H., Curchitser, E., Powell, T. M., and Rivière, P.: North Pacific Gyre Oscillation links ocean climate and ecosystem change, *Geophys. Res. Lett.*, 35, L08607, doi:10.1029/2007GL032838, 2008.
- Feely, R. A., Boutin, J., Cosca, E. C., Dandonneau, Y., Etcheto, J., Inoue, H. Y., Ishii, M., Le Quéré, C., Mackey, D., McPhaden, J., Metzl, M. N., Poisson, A., and Wanninkhof, R.: Seasonal and interannual variability of CO₂ in the equatorial Pacific, *Deep-Sea Res.*, 49(13–14), 2443–2469, doi:10.1016/S0967-0645(02)00044-9, 2002.
- Gruber, N., Gloor, M., Mikaloff Fletcher, S. E., Doney, S. C., Dutkiewicz, S., Follows, J., Gerber, M., Jacobson, A. R., Joos,

- F., Lindsay, K., Menemenlis, D., Mouchet, A., Müller, S., Sarmiento, A. J. L., and Takahashi, T.: Oceanic sources, sinks and transport of atmospheric CO₂, *Global Biogeochem. Cycles*, 23, doi:10.1029/2008GB003349, 2009.
- Gurney, K. R., Law, R. M., Denning, A. S., Rayner, P. J., Pak, B., and Transcom-3-L2-modelers: Transcom-3 inversion intercomparison: Control results for the estimation of seasonal carbon sources and sinks, *Global Biogeochem. Cycles*, 18, GB1010, doi:10.1029/2003GB002111, 2004.
- Hurrell, J. W.: Decadal trends in the North Atlantic oscillation regional temperatures and precipitation, *Science*, 269, 676–679, 1995.
- Jones, D., Collins, M., Cox, P. M., and Spall, S. A.: The carbon cycle response to ENSO: A coupled climate carbon cycle model study, *J. Climate*, 14, 4113–4129, 2001.
- Latif, M. and Barnett, T. P.: Decadal climate variability over the North Pacific and North America: Dynamics and predictability, *J. Climate*, 9, 2407–2423, 1996.
- Latif, M. and Barnett, T. P.: Causes of decadal climate variability over the North Pacific and North America, *Science*, 266, 634–637, 1994.
- Le Quéré, C., Harrison, S. P., Prentice, I. C., Buitenhuis, E. T., Aumont, O., Bopp, L., Claustre, H., Cotrim Da Cunha, L., Geider, R., Giraud, X., Klaas, C., Kohfeld, K. E., Legendre, L., Manizza, M., Platt, T., Rivkin, R. B., Sathyendranath, S., Uitz, J., Watson, A. J. and Wolf-Gladrow, D.: Ecosystem dynamics based on plankton functional types for global ocean biogeochemistry models, *Global Change Biol.*, 11, 2016–2040, doi:10.1111/j.1365-2486.2005.1004, 2005.
- Le Quéré, C., Orr, J. C., Monfray, P., Aumont, O., and Madec, G.: Interannual variability of the oceanic sink of CO₂ from 1979 through 1997, *Global Biogeochem. Cy.*, 14, 1247–1265, 2000.
- Le Quéré, C., Raupach, M. R., Canadell, J. S., Marlat, G., Bopp, L., Ciais, P., Conway, T. J., Doney, S. C., Feely, R. A., Foster, P., Friedlingstein, P., Gurney, K., Houghton, R. A., House, J. I., Huntingford, C., Levy, P. E., Lomas, M. R., Majkut, J. N., Metzl, Ometto, J. P., Peters, G. P., Colin Prentice, I., Randerson, J. T., Running, S. W., Sarmiento, J. L., Schuster, U., Sitch, S., Takahashi, T., Viovy, N., van der Werf, G. R., and Woodward, F. I.: Trends in the sources and sinks of carbon dioxide, *Nat. Geosci.*, 831–836, doi:10.1038/NGEO689, 2009.
- Le Quéré, C., Rödenbeck, C., Buitenhuis, E. T., Conway, T. J., Langenfelds, R., Gomez, A., Labuschagne, C., Ramonet, M., Nakazawa, T., Metzl, N., Gillett, N., and Heimann, M.: Saturation of the southern ocean CO₂ sinks due to recent climate change, *Science*, 316, 1735–1738, 2007.
- Lehodey, P., Senina, I., Sibert, J., Bopp, L., Calmettes, B., Hampton, J., and Murtugudde, R.: Preliminary forecasts of Pacific big-eye tuna population trends under the A2 IPCC scenario, *Progr. Oceanogr.*, 86, 302–315, 2010.
- Lovenduski, N. S., Gruber, N., and Lima, C. D. I. D.: Enhanced CO₂ out gassing in the southern ocean from a positive phase of the Southern Annular Mode, *Global Biogeochem. Cycles*, 21, GB2026, doi:10.1029/2006GB002900, 2007.
- Mantua, N. J., Hare, S. R., Zhang, Y., Wallace, J. M., and Francis, R.: A Pacific interdecadal climate oscillation with impacts on salmon production. *Bull. Amer. Meteor. Soc.*, 78, 1069–1079, 1997.
- McKinley, G. A., Follows, M. J., and Marshall, J.: Mechanism of air-sea CO₂ flux variability in the equatorial Pacific and North Atlantic. *Global Biogeochem. Cycles*, 18, GB2011, doi:10.1029/2003GB002179, 2004.
- McKinley, G. A., Takahashi, T., Buitenhuis, E., Chai, F., Christian, J. R., Doney, S. C., Jiang, M.-S., Lindsay, K., Moore, J. K., Le Quéré, C., Lima, I., Murtugudde, R., Shi, L., and Wetzel, P.: North Pacific carbon cycle response to climate variability on seasonal to decadal timescales. *J. Geophys. Res.*, 111, C07S06, doi:10.1029/2005JC003173, 2006.
- Metzl, N., C. Brunet, Jabaud-Jan, A., Poisson, A., and Schauer, B.: Summer and winter air-sea CO₂ fluxes in the Southern Ocean, *Deep-Sea Res.*, 53, 1548–1563, 2006.
- Midorikawa T., Ishii, M., Nemoto, K., Kamiya, H., Nakadate, A., Masuda, S., Matsueda, H., Nakano, T., and Inoue, H. Y.: Interannual variability of winter oceanic CO₂ and air-sea CO₂ flux in the western North Pacific for 2 decades, *J. Geophys. Res.*, 111, doi:10.1029/2005JC003095, 2006a.
- Midorikawa T., Nemoto, K., Kamiya, H., Ishii, M., and Inoue, H. Y.: Persistently strong oceanic CO₂ sink in the western subtropical North Pacific, *Geophys. Res. Lett.*, 32, L05612, doi:10.1029/2004GL021952, 2006b.
- Newman, M., Compo, G. P., and Alexander, M. A.: ENSO-forced variability of the Pacific Decadal Oscillation, *J. Climate*, 23, 3853–3857, 2003.
- Nigam, S. and Chan, S. C.: On the summertime strengthening of the Northern hemisphere Pacific sea level pressure anticyclone, *J. Climate*, 22, 1174–1192, 2009.
- Obata, A. and Kitamura, Y.: Interannual variability of the air-sea exchange of CO₂ from 1961 to 1998 simulated with a global ocean circulation-biogeochemistry model, *J. Geophys. Res.*, 108, (C11), 3337, doi:10.1029/2001JC001088, 2003.
- Park, G., Wanninkhof, R., Doney, S. C., Takahashi, T., Lee, K., Feely, R. A., Sabine, C. L., Trinanés, J., and Lima, I. D.: Variability of global net sea-air CO₂ fluxes over the last three decades using empirical relationships, *Tellus-B*, 62, 352–368, 2010.
- Patra, P. K., Maksyutov, S., Ishizawa, M., Nakazawa, T., Takahashi, T., and Ukita, J.: Interannual and decadal changes in the air-sea flux from atmospheric inverse modeling, *Global Biogeochem. Cycles*, 19, GB4013, doi:10.1029/2004GB002257, 2005.
- Polovina, J. J., Howell, E., Kobayashi, D. R., and Seki, M. P.: The transition zone chlorophyll front, a dynamic global feature defining migration and forage habitat for marine resources, *Prog. Oceanogr.*, 49, 469–483, 2001.
- Rödenbeck, C., Houweling, S., Gloor, M., and Heimann, M.: CO₂ flux history 1982–2001 inferred from atmospheric data using a global inversion of atmospheric transport, *Atmos. Chem. Phys.*, 3, 1919–1964, doi:10.5194/acp-3-1919-2003, 2003.
- Rodgers, K. B., Freiderichs, P., and Latif, M.: Tropical Pacific decadal variability and its relation to decadal modulations of ENSO, *J. Climate*, 17, 3761–3774, 2004.
- Takahashi T., Sutherland, S. C., Feely, R. A., and Wanninkhof, R.: Decadal change of the surface water pCO₂ in the North Pacific: A synthesis of 35 years of observations, *J. Geophys. Res.*, 111, doi:10.1029/2005JC003074, 2006.
- Takahashi, T., Sutherland, S. C., and Kozyr, A.: Global ocean surface water partial pressure of CO₂ database: Measurements performed during 1968–2006 (Version 1.0). ornl/cdiac-152, ndp-08, Carbon Dioxide Information Analysis Center, 20, 2007.
- Takahashi, T., Sutherland, S. C., Wanninkhof, R., Sweeney, C.,

- Feely, R. A., Chipman, D. W., Hales, B., Friederich, G., Chavez, F., Watson, A., Bakker, D. C. E., Schuster, U., Metzl, N., Yoshikawa-Inoue, H., Ishii, M., Midorikawa, T., Nojiri, Y., Sabine, C., Olafsson, J., Arnarson, Th., Tilbrook, S. B., Johannessen, T., Olsen, A., Bellerby, R., Körtzinger, A., Steinhoff, T., Hoppema, M., de Baar, H. J. W., Wong, C. S., Delille, B., and Bates, N. R.: Climatological mean and decadal changes in surface ocean $p\text{CO}_2$, and net sea-air CO₂ flux over the global oceans, *Deep-Sea Res. Pt. II*, 56, 554–577, 2009.
- Telszewski, M., Chazottes, A., Schuster, U., Watson, A. J., Moulin, C., Bakker, D. C. E., González-Dávila, M., Johannessen, T., Körtzinger, A., Lúger, H., Olsen, A., Omar, A., Padin, X. A., Ríos, A. F., Steinhoff, T., Santana-Casiano, M., Wallace, D. W. R., and Wanninkhof, R.: Estimating the monthly $p\text{CO}_2$ distribution in the North Atlantic using a self-organizing neural network, *Biogeosciences*, 6, 1405–1421, doi:10.5194/bg-6-1405-2009, 2009.
- Thomas, H., Prowe, A. E. F., Lima, I. D., Doney, S. C., Wanninkhof, R., Greatbatch, R. J., Schuster, U., and Corbière, A.: Changes in the North Atlantic oscillation influence CO₂ uptake in the North Atlantic over the past 2 decades, *Global Biogeochem. Cycles*, 22, GB4027, doi:10.1029/2007GB003167, 2008.
- Tjiputra, J. F., Polzin, D., and Winguth, A. E.: Assimilation of seasonal chlorophyll and nutrient data into an adjoint three-dimensional ocean carbon cycle model: Sensitivity analysis and ecosystem parameter optimization, *Global Biogeochem. Cycles*, 21, GB1001, doi:10.1029/2006GB002745, 2007.
- Trenberth, K. and Hurrell, J.: Decadal atmosphere-ocean variations in the Pacific, *Climate Dyn.*, 9, 303–319, 1994.
- Valsala V., Maksyutov, S., and Ikeda, M.: Design and validation of an offline Oceanic Tracer Transport Model for Carbon Cycle Study, *J. Climate*, 21, 2752–2769, 2008.
- Valsala, V. and Maksyutov, S.: Simulation and assimilation of global ocean $p\text{CO}_2$ and air-sea CO₂ fluxes using ship observations of surface ocean $p\text{CO}_2$ in a simplified biogeochemical offline model, *Tellus-B*, 62, 821–840, doi:10.1111/j.1600-0889.2010.00495.x, 2010.
- Vimont, D.: The contribution of interannual ENSO cycle to the spatial patterns of decadal ENSO like variability, *J. Climate*, 18, 2080–2092, 2005.
- Wakita, M., Watanabe, S., Murata, A., Tsurushima, N., and Honda, M.: Decadal change of dissolved inorganic carbon in the subarctic western North Pacific Ocean, *Tellus B*, 62, 608–620, doi:10.1111/j.1600-0889.2010.00476.x, 2010.
- Wanninkhof, R.: Relationship between wind speed and gas exchange over the ocean, *J. Geophys. Res.*, 97, 7373–7382, 1992.
- Zeng, J., Nojiri, Y., Murphy, P. P., Wong, C. S., and Fujinuma, Y.: A comparison of $p\text{CO}_2$ distributions in the northern North Pacific using results from a commercial vessel in 1995–1999. *Deep-Sea Res.*, 49, 5303–5315, 2002.
- Zhang, Y., Wallace, J. M., and Battisti, D. S.: ENSO-like interdecadal variability in the Pacific, *J. Climate*, 10, 1004–1020, 1997.